Efficient response modelling for performance characterisation and risk assessment of ship-iceberg collisions

Abayomi Obisesan and Srinivas Sriramula

Lloyd's Register Foundation (LRF) Centre for Safety and Reliability Engineering, School of Engineering, University of Aberdeen, Aberdeen AB24 3UE, United Kingdom

Corresponding author: Dr Srinivas Sriramula, Email: s.sriramula@abdn.ac.uk; Tel: +44(0)1224272778; Fax: +44(0)1224272497

Efficient response modelling for performance characterisation and risk assessment of ship-iceberg collisions

Abayomi Obisesan and Srinivas Sriramula[1]

ABSTRACT

Unique features of the Arctic region, such as sub-zero temperatures and glacial activities, pose serious risk to ships. The potential for ship accidents requires tailored guidelines for ship-ice interactions which justify the need for a suitable performance and risk assessment model for ships navigating in the Arctic waters. Research on the development of such model is currently limited. In this paper, a conceptual framework is proposed for performance characterisation and quantitative risk assessment of ships in iceberg collisions. The framework focusses on the components required for asset risk computation, such as probabilistic performance measures and ship-iceberg collision probability. The computationally intensive ship-iceberg collision models are captured by efficient surrogate models in performance estimation, while the basic events are linked by a fault tree representation to identify collision probability. The interaction between a double-hull oil tanker and a spherical iceberg is chosen as the reference collision scenario to demonstrate the applicability of the framework. The crushable foam plasticity model for the iceberg material is validated and the response computations are performed using the non-linear finite element software Abaqus®. The presented computation model underlines the significance of different risk components, providing valuable guidance for improving risk-based ship designs.

Keywords: ship collision; structural reliability; risk assessment; iceberg impact; hull damage; numerical simulation

1. INTRODUCTION

The regions of the Arctic are attracting the interest of multinational organisations due to the opening of new ship passages and the availability of large reservoirs of oil and gas. Exploration and exploitation of these regions will not come easy as the environment is characterised by sub-zero temperature and glacial activities, leading to ice formations. The combination of these factors have the potential to cause an increase in accidents such as ship collisions [1]. Due to this reason, ship designers are taking proactive steps to design ship structures that are capable

[1] Corresponding author. Email: s.sriramula@abdn.ac.uk

of withstanding ice loads. These steps require new guidelines for risk-based ship design that would assess potential ship impacts in icy waters.

Two major factors identified as critical during Arctic operations are lack of information on ice conditions and the corresponding inability to predict ice loading on the ship hull [2]. These types of uncertainties can have significant effect on the ship structural response during ice impacts as they influence the response computations. Some typical examples of these parameters are the mass and local geometry of ice bodies, ship displacement, relative velocity and collision angle between the ship and ice formation [2-4]. Hence, uncertainties in ship-ice impact response need to be efficiently characterised for the purpose of quantifying the performance of ship structures and the associated collision risks. According to the probabilistic Formal Safety Assessment (FSA) procedure recommended by the International Maritime Organisation (IMO), possible collision scenarios need to be identified for the quantitative assessment of collision risk to allow for the estimation of the probability of collision scenarios and the associated consequences [5]. In general, risk is evaluated as:

$$Risk = \sum_{i=1}^{n} P_i(Damage) \times Consequence_i \,, \tag{1}$$

where $P(Damage)$ is the probability of damage that considers all potential accident sequences. In the context of a ship collision event:

$$P(Damage) = P(Damage|Collision) \times P(Collision), \tag{2}$$

where $P(Damage|Collision)$ is the probability of damage given a collision and $P(Collision)$ is the probability of a collision. The consequences could be considered in terms of structural, economical, environmental and social effects. The collision probability can be estimated from the construction of logical diagrams, such as fault trees, event trees and Bayesian networks, which involve the relationship of basic events leading to the undesired event. Reddy et al. [6] developed a fault tree, with the associated iceberg quantities as basic events, to estimate the probability of iceberg impacts with offshore structures using a Monte Carlo simulation approach. Korsnes [7] presented the probability of iceberg impact on an offshore structure by estimating the mean annual iceberg production, using an improved iceberg melting and breakdown model. Khan et al. [8] developed a framework for risk assessment of ship transport in the Arctic by constructing a Bayesian network that relates the probability of ship collision with the oil spill consequence. However, the evaluation of the consequence did not relate the loss from oil spill with ship structural damage.

The shared-energy design principle is often employed for the determination of ship structural strength and assessment of related consequences; this means that the results of ship-iceberg collision analysis include significant deformation of both the ship structure and the iceberg [9]. The material of ice has both solid and fluid features that determine its response during loading, such as load-displacement and load-fluid velocity relationships [10, 11]. The consideration of these two models for response characterisation makes ice a highly complicated material thereby making it difficult to accurately capture its deformation mechanism. A simplified approach is usually applied which involves the consideration of short-term, quasi-static loading for ice material behaviour hence, fluid response in ice can be neglected for the assessment [12-15]. If the pressure-area relationship outcome from the approach is verified to be reasonable when utilised under strength design (that is ice deforms only), then the ice material model is also considered sufficient to capture ice behaviour under shared-energy design [13]. The characterisation of structural performance by stochastic modelling has been extensively applied to the case of ship-ship collisions [16-19]. The approach is transferable to ship-iceberg collision analysis, however specific guidance on computationally efficient performance and risk quantification is not available in the literature. Liu et al. [20] performed probabilistic ship-iceberg collision assessment using Bayesian networks by linearising idealised stages of the energy-displacement curve to evaluate the objective function. However, the linearisation procedure may not always represent the energy displacement relation accurately, especially for complex collision cases.

In order to address these limitations, the present study combines the evaluation of the probability of collision scenarios and characterisation of the associated consequences to propose a conceptual framework for the risk assessment of ship-iceberg collisions, as shown in Figure 1 (discussed further in Section 1.2). The study proves the transferability of the framework proposed for ship-ship collisions to other collision variants such as ship-iceberg, ship-bridge, and ship-platform (see [21]). Appropriate probabilistic characteristics of underlying uncertain parameters are identified from the literature. Samples of the variables required for response characterisation are generated using the Latin Hypercube sampling (LHS) apporach. The study also illustrates the characterisation of the plasticity stage of the iceberg material in the nonlinear finite element software, Abaqus®, using the crushable foam model and the result is calibrated against recommended practice. The novelty of the framework relates to the evaluation of efficient response models that characterise ship-iceberg collisions, estimation of the probability of ship structural damage and the evaluation of the causation probability for risk computation. The path relating to the 'Response Surface Modelling Module' of the framework is taken in the present study.

To show the functionality of the framework, a reference collision scenario involving two moving deformable bodies is analysed. These bodies are an iceberg and a double-hull crude oil tanker. Ice formations that may interact with ships vary in terms of production stage and categories. It may be unrealistic to develop tailored ice material models that are peculiar to all types of ice condition. Also, icebergs are known to be highly hazardous due to detection difficulties during navigation [22-24]. Therefore, the scope of the present study focuses on iceberg modelling and interaction with ships. The consequence considered is defined as the rupture of the asset which could lead to flooding of the damaged compartment, and ultimately impeding on the asset intact stability. The focus of the present study is the assessment of the primary consequence to support decisions on the design process of ship structures in risk-based designs. The consequence is assessed in terms of the internal energy dissipated by the ship structure during collision using the non-linear finite element software, Abaqus®.

Kriging response surface model is used to formulate a generic mathematical relationship between the input random variables and the response. The development of ship response function using Kriging model is done using MATLAB®. For the purpose of assessing the risk to the reference ship structure, structural reliability analysis is performed by using the evaluated Kriging model in the First and Second Order Reliability Methods (FORM/SORM) to estimate $P(Damage|Collision)$. The collision probability $[P(Collision)]$ is evaluated by considering the logical relationship between possible basic events leading to the accident using fault tree analysis (FTA). For the present study, the number of possible ship-iceberg collisions is calculated from the iceberg impact analysis presented by Eik and Gudmestad [25] for the Shtokman region. The focus of the present study is for risk computation in terms of structural consequences only.

The modules used for the categorisation of elements of the proposed framework are discussed in Section 1.2. Before going into the assessment of the reference collision scenario, a detailed description and validation of the iceberg material model is given in Section 2. Section 3 discusses the numerical evaluation of the structural consequence and capacity of the reference double-hull oil tanker in a collision scenario involving an iceberg. Hence, structural response that is vital for asset risk computation is identified in this section. The probabilistic characteristics of the input random variables identified for the ship-iceberg collision scenario are described in Section 4. In Section 5, the Kriging surrogate model of the non-linear finite element analysis models is developed for response characterisation. The application of the Kriging model for the evaluation of $P(Damage|Collision)$ along with collision probability computation are discussed in Section 6. Finally, the asset risk computations associated with the studied ship-iceberg collision scenario are demonstrated in Section 6.

1.1 Proposed framework for ship performance and risk computation in iceberg collisions

The developed framework can be categorised into four main modules (Figure 1); ship mechanics module, uncertainty characterisation module, response surface modelling module and performance and risk computation module. The basis for the ship mechanics module is to define the reference ship-iceberg collision scenario and to set the performance targets expected of ship structures to achieve when involved in collisions. These performance targets can be linked with ship responses to develop the failure criteria to which ship structural performance can be assessed.

The objective or performance function of the ship-iceberg collision analysis can then be formulated from either simplified analytical models (SAM) or response surface modelling. The former applies to the analysis of the structural mechanism of the reference collision scenario response by categorising the response in stages with respect to structural member contributions to the total ship response (see [26]). The mathematical relationship between the categorised ship structural response for each stage and input random variables of the reference ship and iceberg can then be evaluated from the first principles. Having a closed-form performance function from SAM is advantageous. In practice, SAMs representing ship structural behaviour are usually in complex forms which could feature high nonlinearity and correlation between input variables [27-29]. Also, the evaluated performance function may be implicitly defined and may not be suitable for tools utilised for performance measures. In such cases, response surface modelling techniques are applied. The outcome of these techniques is the evaluation of surrogate models that provide a simplified way of assessing the reference ship response in the place of computationally intensive models.

Also, there is a possibility of having ship-iceberg collision analysis where closed form performance functions and surrogate models are not applicable. In such cases, response data from the propagation of uncertainty probabilistic characteristics through the '*Python scripting +FEM*' sub-module can be directly applied to sampling-based methods, such as Monte Carlo Simulations, for the computation of performance measures. The automation of the deterministic nonlinear finite element analysis software, Abaqus®, and the stochastic characterisation of ship structural performance are the basis of the proposed framework making it possible to transform capabilities of ship collision analysis to compute performance measures and risks.

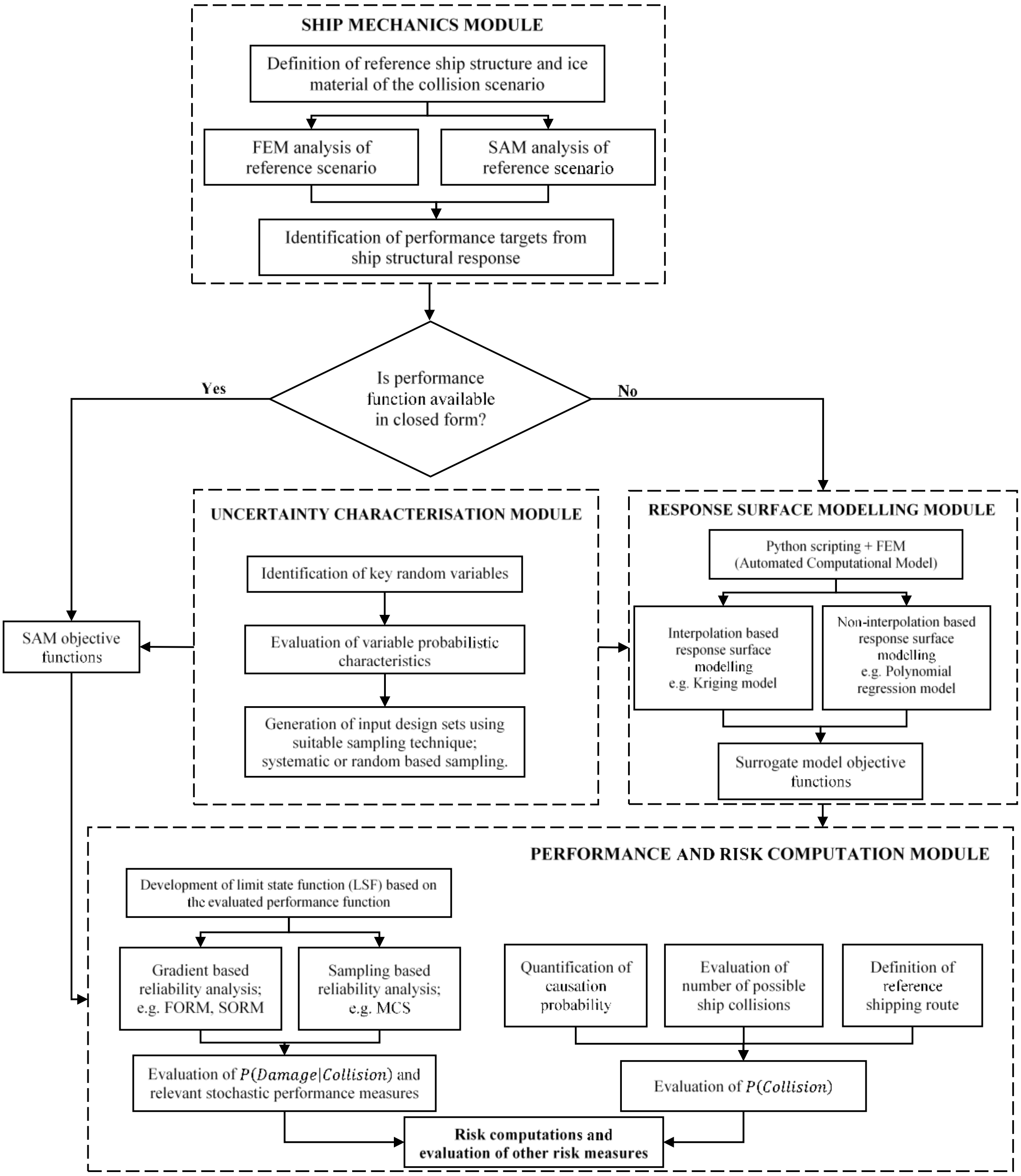

Figure 1. Proposed framework for stochastic performance and risk assessment of ship-iceberg collisions.

2. ICEBERG MATERIAL MODEL

The deformation of ice is influenced by characteristics such as porosity, ambient temperature, salinity, strain rate and grain size. As mentioned earlier, a time-independent load and displacement relationship is usually considered as the solid ice material behaviour in ice mechanics due to the 'short-term' loading period of ice in ship impacts [10-12]. Hence, the material behaviour of ice is comparable to that of steel as it exhibits deformation mechanism that ranges from ductile to brittle under compression followed by failure or, in simple terms, softening. The stress-strain model of ice is divided into stages to characterise the processes of material mechanism. The stress and strain relationship at the first stage of iceberg deformation is linear, thereby satisfying the Hooke's law of elasticity. The critical transition from the elastic to plastic state follows an increase in ice strength as well as hydrostatic pressure and the constitutive relations at this stage can be characterised by a yield surface function [14]. At the plastic state, a selected flow rule is defined with the yield surface to characterise the constitutive relations up until material failure.

The yield surface function and other ice material model parameters useful for numerical modelling are usually formulated based on experimental results. The common laboratory tests for ice are triaxial compression, uniaxial testing, flexure and indentation [30, 31]. It was observed from the result of these experiments that the parameters of yield surface are functions of temperature and strain-rate. The temperature of icebergs varies significantly with depth due to their low thermal conductivity; temperature is constant at depth close to the iceberg core while the surface temperature varies with seasonal air temperature [32]. The influence of strain-rate on ice material behaviour is well established from experiments. It has been observed that the strength of iceberg increases as the strain rate increases up to $5 \times 10^{-3} s^{-1}$ [31, 33], after that the strength was observed to reduce at higher strain rates resulting in brittle failures.

Derradji-Aouat et al. [34] concluded that icebergs experience ductile failure at low strain rates ($< 10^{-3}s^{-1}$) and brittle failure at high strain rates ($> 10^{-3}s^{-1}$).

2.1 Ice yield surface modelling

The constitutive models of ice that have been developed in the literature comprise at least one of the following yield surfaces; Tsai-Wu [13, 31], crushable foam [35, 36], Drucker-Prager and Mohr-Coulomb [37]. The theory of Tsai-Wu yield surface is well detailed in the references provided as an elliptical yield envelope in hydrostatic pressure stress-deviatoric stress second invariant plane. The study by Gao et al [38] analysed the influence of iceberg shapes on the ship-ice interaction response using two different ice material models; the Tsai-Wu and crushable foam models. They found out that the collision model responses are sensitive to the iceberg shape when the Tsai-Wu model is employed while the responses are not sensitive to the iceberg shape when the crushable foam model is applied. Therefore, it is more reasonable to apply the crushable foam plasticity model for the present study. Also, the model can be easily adapted to numerical simulations as the representative parameters are obtainable from experimental based yield surfaces developed in the literature. The yield surface of the crushable foam model is an ellipse in the hydrostatic pressure stress-Von Mises stress ($p - q$) plane and is defined as [39]:

$$f(p, q) = \sqrt{q^2 + \alpha^2(p - p')^2} - B = 0, \tag{3}$$

where $p = -\sigma_{kk}/3$ is the hydrostatic pressure stress, $q = \sqrt{\frac{3}{2} s_{ij} : s_{ij}}$ is the Von Mises stress, α is the shape parameter of the ellipse, p' is the location parameter that specifies the centre of ellipse on the p −axis and B is a scale parameter that defines the size of the ellipse on the q −axis. The scale parameter that defines the ellipse size on the p −axis is denoted as A. The relationship between these parameters can given as:

$$A = \frac{|p_{min}| + p_{max}}{2}, \tag{4}$$

$$B = q_{max}, \tag{5}$$

$$\alpha = \frac{B}{A}, \tag{6}$$

$$p' = \frac{p_{max} - p_{min}}{2}, \tag{7}$$

where p_{min} and p_{max} are the lower and larger roots of the $p - q$ plane, respectively, and q_{max} is the maximum point of the yield surface on the $q -$axis. The Abaqus® crushable foam plasticity model can be defined using two parameters:

$$k = \frac{\sigma_c^o}{p_c^o}, \tag{8}$$

$$k_t = \frac{p_{min}}{p_c^o}, \tag{9}$$

where k is the yield stress ratio for compression loading, k_t is the hydrostatic yield stress ratio, p_c^o is the initial yield stress in hydrostatic compression and σ_c^o is the initial yield stress in uniaxial compression which is equal to the point where the yield surface intersects the $q -$axis. It is observed that all the parameters of the crushable foam plasticity model are derivable from the constructed shape of the yield surface except for p_c^o. However, the value of p_c^o can be estimated from the relationship between the shape parameter and the yield stress ratios:

$$\alpha = \frac{3k}{\sqrt{(3k_t + k)(3 - k)}}. \tag{10}$$

It is worth noting that the yield surface function defined in Equation 3 is isotropic if the location parameter has a zero value and $p_{min} = -p_{max}$. This means that an isotropic plastic-hardened ice material will have the centre of its yield surface at the origin of the $p - q$ plane. Derradji-Aouat [33] developed yield surfaces from the result of triaxial tests performed by Gagnon and Gammon [31]. The tests were carried out by compressing glacier ice at confining pressures from 0 to 13.79 MPa, between strain rates of $5 \times 10^{-5}\text{s}^{-1}$ and $5 \times 10^{-2}\text{s}^{-1}$ at varying temperatures. Parameters of the yield surface proposed by Derradji-Aouat [33] are used to characterise the crushable foam plasticity model of the present study as the yield surface validates the ice material model. The parameters of crushable foam plasticity model for ice material are listed in Table 1. The corresponding yield surface derived using the crushable foam function is shown in Figure 2.

Table 1. Crushable foam plasticity model parameters.

Parameter	**Value**
Minimum value of p −axis, MPa	-10
Maximum value of p −axis, MPa	100
Ellipse size on q −axis, MPa	14.39
Compression yield stress ratio	1.49
Hydrostatic yield stress ratio	1.79
Strain rate, s^{-1}	4.4×10^{-3}
Ice temperature, $°C$	-11

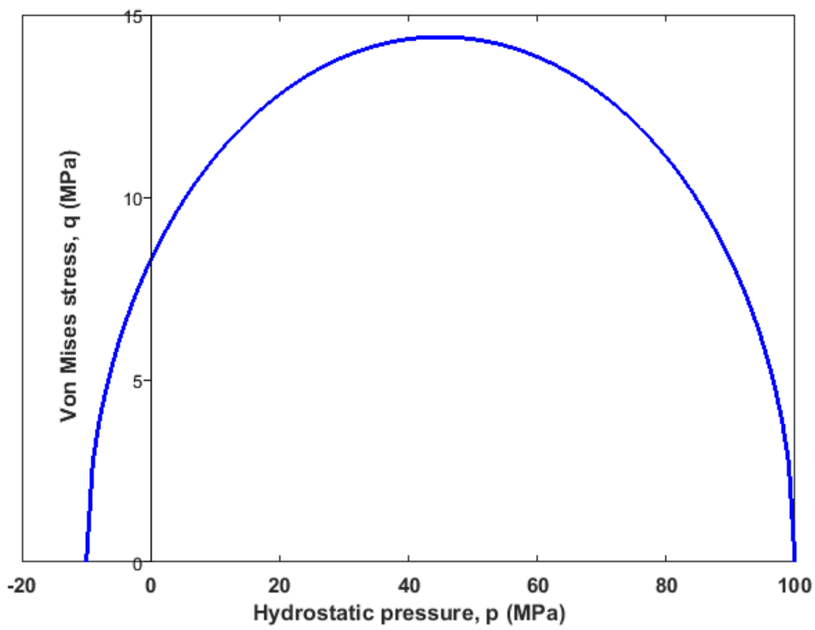

Figure 2. Iceberg material yield surface curve.

2.2 Hardening and damage modelling

As the deformation of the iceberg ice material transits into the plastic state, the size and shape of the yield surface evolves. This evolution is captured in the material response using the hardening model which can be characterised by the yield stress and volumetric plastic strain relationship in uniaxial loading. Volumetric strain refers to the measure of volumetric deformation of ice as its porosity falls under high pressure which is often measured in triaxial tests from the displaced fluid volume in a triaxial cell [40]. At a constant confining pressure, the volumetric strain can be calculated from:

$$\varepsilon_v = -\ln\left(\frac{V}{V_0}\right), \tag{11}$$

where V_0 is the original sample volume and V is the current sample volume. Gagnon [35, 36] estimated the stress-volumetric strain relations for crushable foam models using data from lab and field experiments and found that the calibrated stress-volumetric strain relations were in good agreement with the test results. Kim et al. [41] updated the stress-volumetric strain relations proposed by Gagnon to achieve the saw-tooth loading pattern of ice observed from experimental studies. The updated stress-volumetric strain relations are used in the present study to characterise hardening in ice material properties as it provides a better representation of ice spalling deformation. The stress-volumetric strain curve is shown in Figure 3.

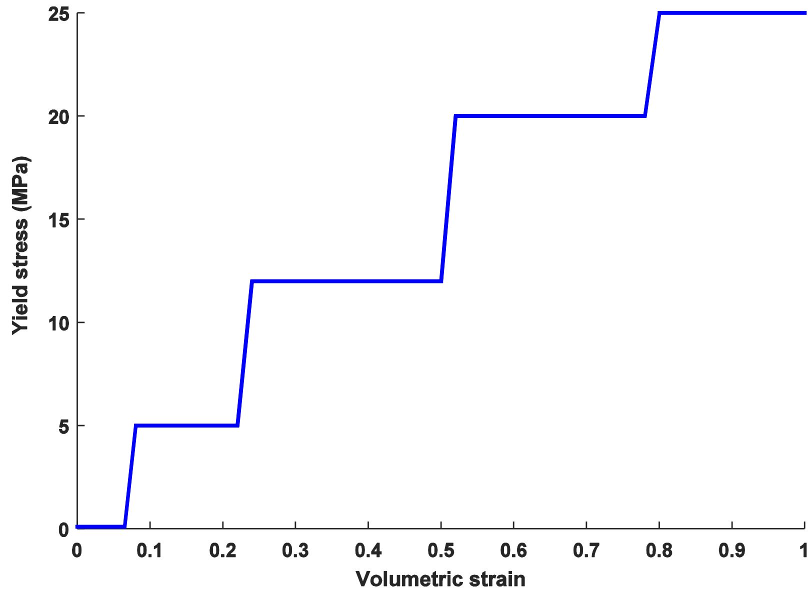

Figure 3. Volumetric strain-yield stress of the crushable foam hardening model.

As mentioned earlier, the mode of failure of iceberg can be compared to that of ductile metal with failure mechanisms such as microcrack formation and shear band localisation leading to ductile and shear fracture, respectively; other mechanisms include dislocation slip and grain boundary sliding [31, 42]. Ice failure is identified in the ice material model once the stress state falls below the plasticity representative that is, the tensile strength. Liu et al. [13] proposed an empirical, user-defined failure criterion that relates the ice stress state and its failure strain as follows:

$$\varepsilon_f = \varepsilon_0 + \left(\frac{p}{p_{max}} - 0.5\right)^2, \tag{12}$$

where ε_0 is the initial failure strain, p_{max} is the larger root of the yield function and p is the pressure. Failure is activated in the ice model when the pressure value drops below the cut-off pressure or the tensile strength. Based on trial simulation results of the crushable foam application, numerical simulations with values 0.01 and 8 MPa for ε_0 and the cut-off pressure, respectively, are found to compare well with recommended practice. This is discussed in the next section.

2.3 Validation of iceberg numerical model

The aim of the present study is to perform a quantitative risk assessment of iceberg impact on ship structures. Such impacts are classified as Abnormal Level Ice Events (ALIE) according to the International standard Organisation (ISO) 19906 classifications for arctic offshore structures [43], corresponding to the Accidental Limit State (ALS) designs for ships and offshore structures. Hence, there is the need to calibrate the developed iceberg ice material model against the recommended practice. This practice involves the comparison of the resulting pressure-area curve with the ISO 19906 standard. The pressure-area curve provides knowledge of the localised ice load as the shape of the contact area and pressure distribution in ice varies. The pressure-area relationship given by the ISO standard and used for calibration of the developed ice model in the study is given as:

$$P = 7.4A^{-0.7}. \quad (13)$$

The ISO pressure-area relationship was found to be a reasonable fit to the field data obtained from experiment with multi-year floe and relatively small ice features. However, the model has been found to compare well with ship-iceberg impact models in the literature [13, 38].

In this paper, a numerical study is performed to determine the maximum contact pressure over actual contact areas. For the sake of comparison, the model geometry is similar to the numerical study done by Liu et al. [13] in which pressure-area relationship was derived based on the Tsai-Wu function representation of the same yield surface used in the present study. The studied collision scenario involves a conically-shaped iceberg and a rigid plate, as shown in Figure 4. The explicit software Abaqus® is used to carry out the simulation. The density of ice is specified as $900\ kg/m^3$ with the elastic property characterised using Young's modulus and poisson ratio values of $9.0\ GPa$ and 0.0, respectively. The iceberg model is meshed using a C3D8R element, which is an 8-noded solid element with reduced integration. The mesh size of 0.2m is applied for the iceberg. The crushable foam plasticity and ductile damage models are defined to model iceberg material behaviour, as discussed earlier. The loading is displacement-controlled which defines the $3.0\ m$ displacement of the rigid plate at a $3.0\ s$ time step. The initial contact area, which is the surface area of the iceberg in contact with the rigid plate is varied to calculate the maximum contact pressure for eight different values of the contact area. The maximum contact pressure is calculated from the average pressure at various stages of ice deformation with respect to the initial contact area.

The simulation results are validated by comparing the derived pressure-area curve with the recommended ISO curve as well as with the pressure-area relationship derived by Liu et al. [13] in Figure 5. Unlike the Tsai-Wu function that agrees well with the ISO curve when the contact area value is less than 0.5 m^2, it can be observed that the crushable foam function compares with the ISO curve better especially at contact area values greater 0.5 m^2.

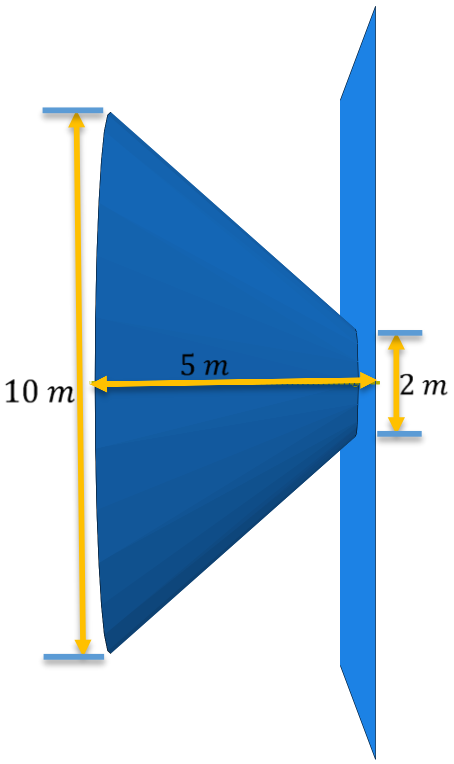

Figure 4. Geometric dimensions of iceberg-rigid plate collision model.

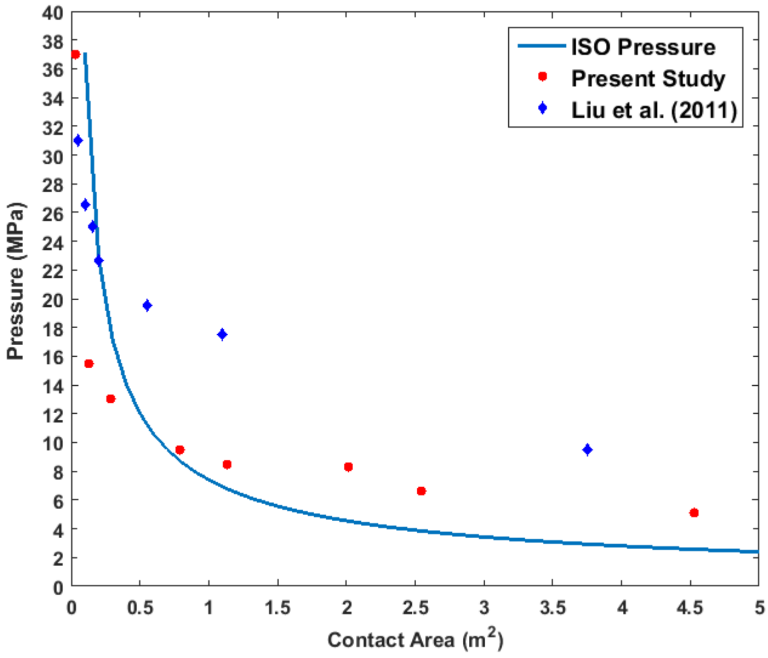

Figure 5. Comparison of the maximum pressure – contact area relationships.

3. NUMERICAL MODEL OF THE REFERENCE SHIP-ICEBERG COLLISION SCENARIO

For the purpose of showing the functionality of the proposed risk computation model for ship-iceberg collisions, a reference collision scenario is studied. In this section, the collision structural consequences and capacity of a 105,400 DWT double-hull tanker in a collision with an iceberg are evaluated. The geometrical properties of the tanker is adapted from the struck vessel considered in the ship collision analysis performed by Lutzen [44]. The internal mechanics of the selected scenario are investigated and the responses are analysed using non-linear finite element analysis. The mid-ship hull area is one of the key parts of the ship structure that frequently experience ice impacts during voyage [14]. For this reason, the ship hull section is modelled in the present study. To reduce computational costs, the full-scale double-hull support structure of the cargo hold section between two transverse bulkheads is modelled. The material for the double-hull is mild steel. Other main dimensions of the double-hull are presented in Figure 6 and Table 2. The geometry of the iceberg in the region directly involved in the collision is vital for effective assessment of the ship local deformation. A spherical-shaped iceberg with a radius value of 5 m is considered in the present study. The iceberg shape is in line with recommendations and assumptions for mean iceberg model shapes [45, 46]. However, half of the iceberg shape is modelled in the present study as the other half would have no contact with the reference ship throughout the simulation. Hence, the reference collision scenario can be described as a $100°$ angle collision between a double-hull oil carrier and a spherical iceberg with contact occurring mid-way along the longitudinal direction of the double-hull structure, as shown in Figure 7.

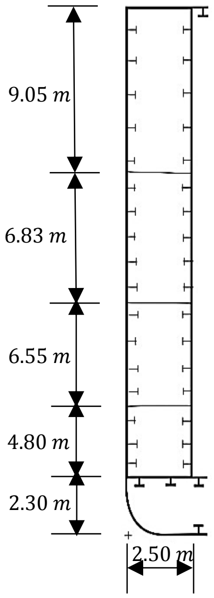

Figure 6. Section view and dimension of the reference ship.

Table 2. Properties of the reference ship.

Geometric properties		Material properties	
Length (m)	274.0	Density (kg/m^3)	7850
Breadth (m)	48.0	Young's modulus (MPa)	210
Depth (m)	29.53	Poisson's ratio	0.30
Displacement (t)	105,400	Yield stress (MPa)	235
Draught (m)	17.07	Strain at yield point	0.003
Cargo hold length (m)	29.60	Fracture strain	0.20
Stiffener dimension (mm)	$400 \times 100 \times 13/18$	Failure displacement	0.08
Frame spacing (m)	3.70	Typical element dimension (m)	0.38

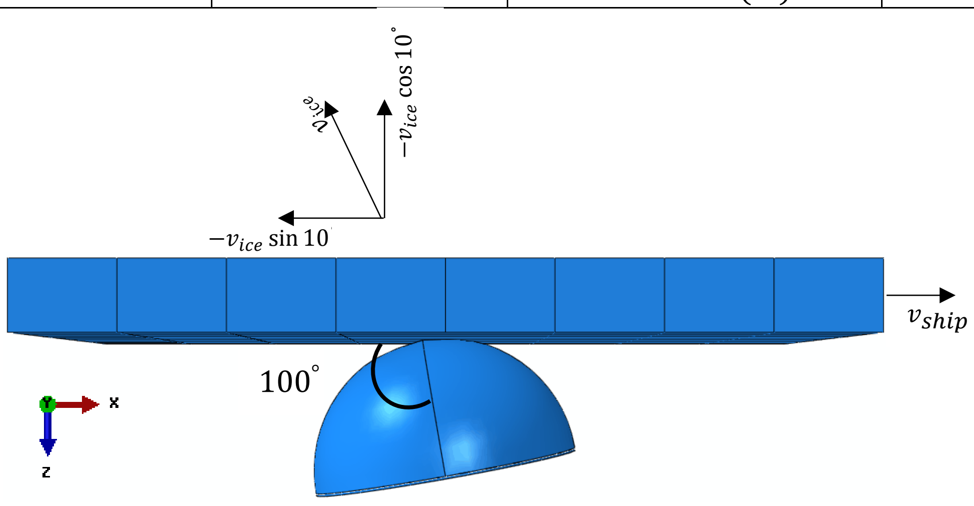

Figure 7. Plan view of the reference collision scenario showing the ship and iceberg velocities.

The collision scenario is simulated using the explicit software Abaqus®. A rigid plate is attached to the base of the iceberg model to aid iceberg displacement. A velocity of $0.5\ m/s$ is assigned to the iceberg while the double-hull is modelled to have a velocity of $2.0\, m/s$. These velocities are representative of the condition at the instant of impact. The material properties of the iceberg model are defined as per the discussion in Section 2. The material plasticity model is defined by the power law as:

$$\sigma = k\left(\varepsilon_y + \varepsilon^p\right)^n, \tag{14}$$

where ε_y and ε^p are the strain at yield point and effective plastic strain, respectively, k and n are the material constants with values 650 and 0.23, respectively. Other material properties of the double-hull are presented in Table 2. To reduce the computational cost of the simulation, the iceberg penetration distance at which the simulation is set to stop is equal to the spacing between the ship inner and outer hull, that is $2.50\, m$. The resulting damage to the double-hull and the iceberg at the end of the simulation is shown in Figure 8. The structural members of the double-hull are observed to undergo substantial plastic deformation prior to the outer hull fracture. Although deformation of several structural members contributes to the resistance of the double-hull, the deformation is still found to be localised within the contact region relative to the ship and iceberg motions. The iceberg surface area is observed to reduce as the collision progresses. However, only few elements failed in the iceberg model showing the underlying strength of the material.

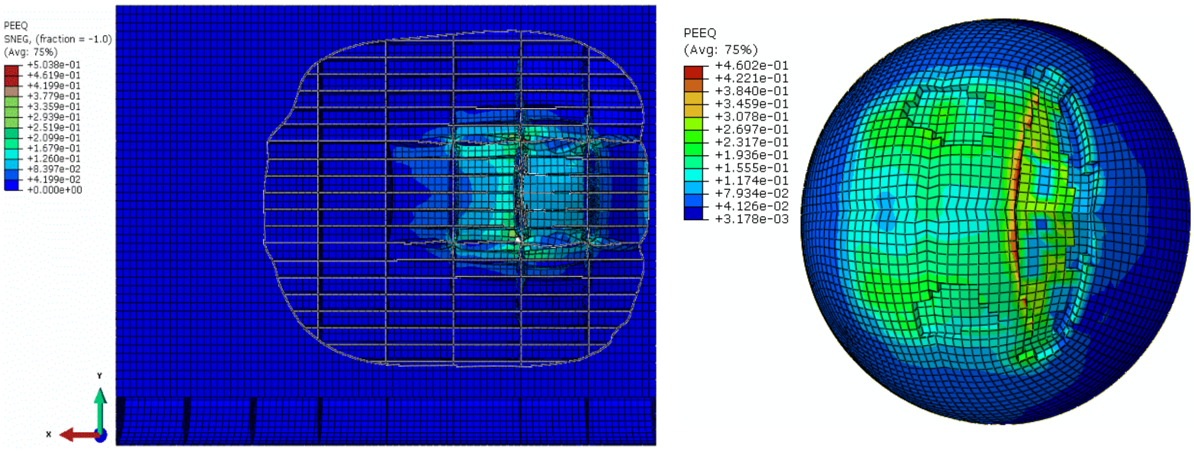

Figure 8. Section views of the collision simulation showing the double-hull and iceberg deformation.

The force-penetration relationship for the iceberg and double-hull structures is shown in Figure 9. The progressive deformation mechanism is observed for the iceberg with the occurrence of a sharp decline in load after a steady load increase. At the beginning of the collision, the iceberg deforms more than the double-hull with relatively higher impact force up until a penetration distance of 1.39m after which more iceberg elements are observed to fail. The observed instance coincides with the establishment of contact at a cruciform junction of the double-hull structural members. The outer hull experienced significant membrane stretching until the occurrence of rupture at a penetration value of 2.32m. The effect of considering the impact of two non-static, deformable bodies is evident in the shared energy dissipation between the iceberg and the double-hull structure, as shown in Figure 10. The energy absorbed by the double-hull until the onset of outer hull fracture, that is 46.05MJ, is also highlighted. The collision energy at the end of the simulation is 93.54MJ with the iceberg and the double-hull absorbing approximately 33% and 67%, respectively, of the total energy. The extent of damage to the double-hull is measured by considering the volume of damaged structural members that undergone plastic deformation during the collision. The damaged volume (Vol_D) is estimated from the simulation results as the summation of the volume of double-hull elements with strain values (ε_i) exceeding that at yield point (ε_y) as:

$$Vol_D = \sum_{i=1}^{n} Vol_i(\varepsilon \geq \varepsilon_y). \tag{15}$$

Hence the damaged volume of the double-hull at the onset of outer hull fracture and at the end of the simulation are 3.99 m^3 and 4.27 m^3, respectively. The double-hull response values at the specified simulation stages are representative of the ship capacity as well as its structural consequences due to the collision event. The values are relevant to compute the risk associated with the ship-iceberg collision.

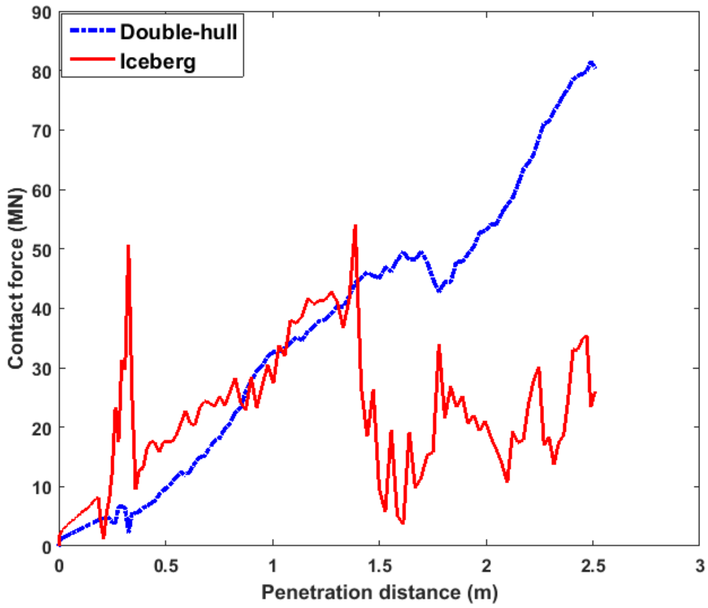

Figure 9. Force-penetration curves of the collision simulation.

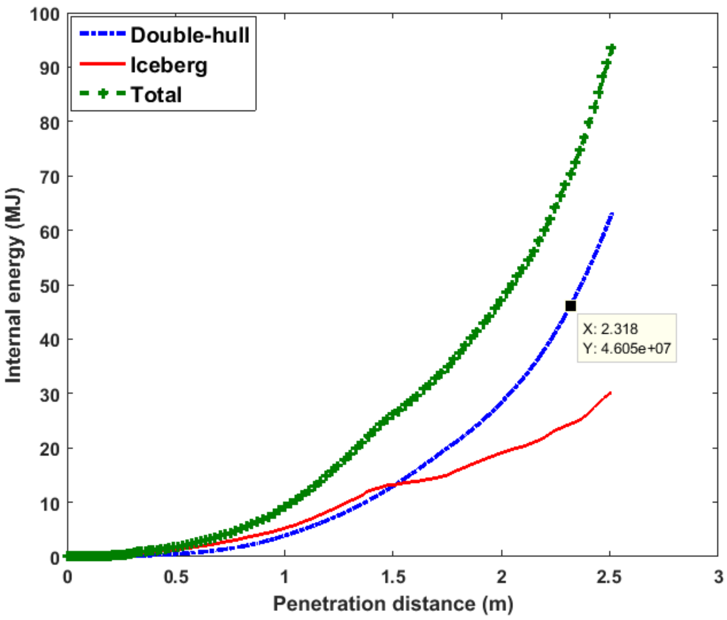

Figure 10. Energy-penetration curves of the collision simulation.

4. UNCERTAINTY MODELLING OF THE STRUCTURAL RESPONSE

As mentioned in Section 1, Ship collision response is characterised by uncertainties due to the variability of parameters influencing the collision scenario. In order to quantify response uncertainties in a probabilistic framework, multiple sampling sets are generated with respect to the probabilistic characteristics of the input random variables. More specifically, the prominent input random variables are: ship displacement, ship draught, collision angle, impact location, iceberg local geometry, the mass and velocity of the iceberg and ship. The probabilistic quantification of these variables is performed using historical data and accident statistics. A brief description of these variables is provided in this section.

4.1 Iceberg mass distribution

There is a large amount of literature in estimating the probability distributions for iceberg mass. This is usually done relative to either the length or width of the iceberg [47] because data are usually collected based on ship sightings, aircraft or satellite imagery [48]. Fuglem [4] evaluated the iceberg waterline length (L_{ice}) function as a sum of two exponential distributions defining larger and calved icebergs based on the hypothesis that the number of icebergs with length greater than 20m is approximately equal to those whose lengths are between 5 and 20m. In the present study, it is assumed that the larger and calved icebergs are statistically independent, this means that zero covariance is used in their representation. The distribution for iceberg length is then given as:

$$f(L_{ice}) = 0.43[0.017\exp-(0.017L_{ice})] + 0.57[0.125\exp-(0.125L_{ice})]. \qquad (16)$$

Based on experimental data, the empirical model that relates iceberg length and its mass was presented by Ralph et al. [49] as:

$$M_{ice} = aL_{ice}^3, \qquad (17)$$

where the coefficient a is approximately $0.331\,t/m^3$. The equation was found to be a reasonable fit for estimating iceberg mass based on the analysis of several data sources. By evaluating the equations, the iceberg mass in the present study is characterised using the exponential distribution with a parameter value of 2.50×10^{-5}.

4.2 Iceberg velocity distribution

The velocity of iceberg is dependent on the wind drag and the drifting wave actions at the moment of collision. Fuglem [4] developed a model for the velocity by considering the marginal influence of iceberg sizes, wind and current drag forces on the iceberg drifting velocity. The model and two-parameter Weibull distribution representation were found to agree reasonably well with observed data. The corresponding shape and scale parameters of the Weibull distributions are 1.5 and 0.32, respectively [20].

4.3 Ship velocity distribution

The quantification of the variability in ship velocity is well detailed for ship-ship collisions. However, limited information is available with respect to the present study. The study by Leira et al. [2] estimated the distribution for ship speed based on its influence on the strain recorded on a vessel due to ice loading. However, the speed data considered were the mean values when the highest fractions of ice load acted on the vessel for defined periods of time. Due to limited historical data on ship-iceberg collisions, the probabilistic characteristics of ship velocity for ship-ship collisions are considered for the present study. The study by Brown [17] collated historical ship collision data to model ship-ship collision scenario parameters. The Weibull distribution was found to be a good fit for the velocity of a striking tanker ship with the shape and scale parameters of 2.2 and 6.5, respectively. The characteristics of this Weibull distribution are selected in the present study to model the velocity variable of the considered double-hull tanker.

4.4 Ship displacement distribution

The type of ship in collision analysis is important for the uncertainty quantification of ship displacement. This is because the likelihood of collision involving a particular type of ship is different from the other and the loading condition at the onset of collision varies. There is limited information about the type and displacement of ships navigating in the Arctic region. Based on data from world casualty statistics, Brown [17] modelled ship displacement distributions using different two-parameter Weibull models for five ship categories. Liu et al. [20] assumed a uniform distribution with equal encounter probabilities and specific displacement values for five ship categories navigating the Arctic seas. This assumption is also applied to the present study. Hence, ship displacement variable is characterised using Uniform distribution with lower and upper parameters of $50{,}000t$ and $150{,}000t$, respectively.

4.5 Collision angle distribution

Statistical information regarding the angle made between the striking ship and the iceberg at the moment of impact is not available in the literature. In this respect, data available for ship-ship collisions are considered instead. Brown [17] characterised the collision angle made by a striking ship with respect to a struck ship using a Normal distribution based on the historical data from global accident investigations. Since collision angle referenced the striking ship, the same data could be applied to ship-ice interactions. Hence, the result of Brown's characterisation of collision angle variable is adopted for the present study. The mean and standard deviation parameters of the collision angle, following a Normal distribution were found to be $90°$ and $28.97°$, respectively. The unit for collision angle is measured in radian for the present study.

4.6 Impact location and ship draught distributions

The longitudinal impact location and the ship draught are key parameters that determine the location along the ship structure where the impact would occur. At present, specific information about these variables is not available with regards to ship-iceberg collisions. The longitudinal impact location on the striking ship is evaluated as the ratio of the distance between the impact point and the ship foremost point and the length of the ship. The probabilistic characteristics provided for ship-ship collisions by Youssef et al. [3] are applied for impact location in the present study; the Weibull distribution with the shape and scale parameters of 2.6 and 0.6, respectively, is applied.

The ship draught is the measure of the distance between the waterline and the hull bottom. This means that the measure of draught at the time of impact will be dependent on the ship displacement and sea state. The study by Brown [17] presented a displacement-dependent power law to represent ship draught with respect to striking ship type. The equation to derive the draught of tanker ship is given as:

$$D_{ship} = 3.98{\Delta_{ship}}^{0.13}, \tag{18}$$

where Δ_{ship} is the ship displacement in tonne. Hence, the striking ship draught can be modelled by a uniform distribution with lower and upper parameters of $17.0m$ and $19.70m$, respectively. The variability in the geometry of the colliding iceberg at the local contact with ships is also a key parameter influencing ship structural response.

A deterministic iceberg geometry is considered in the present study that is, the hemispherical shape and geometric properties of the iceberg in the reference collision scenario. Although several geometries have been considered in the literature (e.g. [38, 50-52]), there is a need for more research into their categories and probabilistic characterisation. The probabilistic characteristics of all the input random variables considered for the ship-iceberg collision study are presented in Table 3.

Table 3. Probabilistic characteristics of the input random variables.

Variable	**Distribution**	**Parameter**	**Mean**	**COV**
Iceberg mass, M_{ice}	Exponential	$\lambda = 2.50 \times 10^{-5}$	$39.56kt$	0.32
Iceberg Velocity, v_{ice}	Weibull	$\alpha = 1.50, \beta = 0.32$	$0.29\,m/s$	0.68
Ship displacement, Δ_{ship}	Uniform	$a = 50kt, b = 150kt$	$100kt$	0.29
Ship velocity, v_{ship}	Weibull	$\alpha = 2.20, \beta = 6.50$	$2.96\,m/s$	0.48
Collision angle,θ	Normal		$1.57\,rad$	0.32
Impact location,I_l	Weibull	$\alpha = 2.60, \beta = 0.60$	0.54	0.42
Ship draught, D_{ship}	Uniform	$a = 17.0m, b = 19.70m$	$18.83m$	0.09

5 RESPONSE SURFACE MODELLING

Due to the high computation requirements of collision response models and the need for efficient performance and risk assessment of ship structures, surrogate models are developed by establishing a mathematical relationship between input random variables and the ship response. Discussions in this section describe the procedures for evaluating surrogate models to characterise ship response when in collision with an iceberg that is, the procedures of the 'Response Surface Modelling Module' of the proposed framework (see Figure 1).

5.1 Stochastic finite element analysis

The first step in the model evaluation involves the construction of samples, called input design sets in the present study. There are several sampling techniques but it is vital to ensure that the generated sets reflect the most probable sampling range of the input random variables. Design of experiment (DoE) techniques, such as the central composite design (CCD) and Box-Behnken design (BBD), may be employed for very sensitive studies that require more emphasis on the centre/mean and the neighbouring regions of specific random variables [53-56].

In the present study, Latin Hypercube sampling (LHS) technique is used to generate the input design sets due to its low discrepancy property [57, 58]. The probability distribution of each input parameter is divided into N intervals of equal probability. One sample is then drawn from each interval for each input parameters, by ensuring that the drawn samples are the only ones from their axis-aligned hyperplane. Therefore, the number of generated input design sets is equal to the number of intervals N. LHS requires the specification of the minimum and maximum values of the random variables to serve as sample boundaries. For the present study, these values are prescribed based on the guidelines from literature [2-4]. For variables whose boundary values are not available, expert opinions are followed by evaluating the minimum and maximum values from $\mu_x - 3\sigma_x$ and $\mu_x + 3\sigma_x$, respectively; where μ and σ are the mean and standard deviation of the random variable, x, respectively. The resulting minimum and maximum values are assumed to be boundaries for approximately 99% of variable occurrence probabilities. The boundary values presented in Table 4 are used to generate 90 design sets using the LHS technique in the present study. These design sets are presented in the model shown in Figure 11. The model is a lower triangular matrix which pairs the considered variables in order to show their relationship and the normal distribution of the input design set.

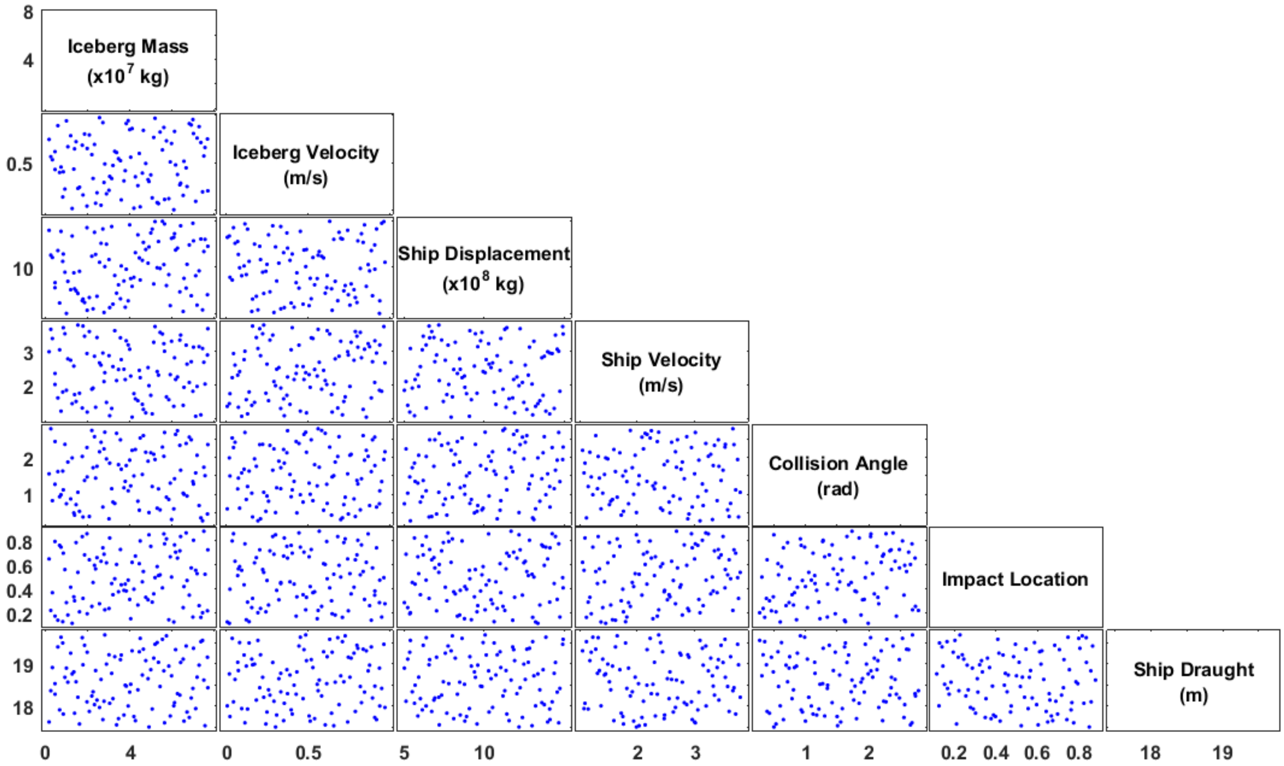

Figure 11. Latin hypercube sampling model.

Table 4. Bounds of the input random variables.

Variable	Minimum	Maximum	Reference
Iceberg mass, M_{ice}	$1.58kt$	$77.54kt$	
Iceberg Velocity, v_{ice}	$0\,m/s$	$0.98\,m/s$	[4]
Ship displacement, Δ_{ship}	$50kt$	$150kt$	
Ship velocity, v_{ship}	$1.03\,m/s$	$3.81\,m/s$	[2]
Collision angle, θ	$0.26\,rad$	$2.79\,rad$	[3]
Impact location, I_l	0.11	0.88	[3]
Ship draught, D_{ship}	$17.50m$	$19.70m$	

Simulation of the ship-iceberg collisions, with respect to the generated input design sets, are carried out using python scripts through the python development environment (PDE) interface available in the Abaqus® software. The integration of python scripting and Abaqus®, called automated computational model (ACM), is the function that begins the procedure for surrogate model evaluation as indicated in the 'Response Surface Modelling Module' of Figure 1. The automation of the non-linear finite element model allows for a programmable analysis of multiple computations and desired responses in a controlled loop. Further details about this computation are available in Obisesan et al. [26]. A histogram plot of the ship internal energy after impact is shown in Figure 12. The recorded internal energy is observed to be between 1361.63J and 180.93MJ. It is estimated that the energy value set of 0-20MJ occur the most and they correspond to ship-iceberg collision with a penetration distance reaching approximately 1.7m, according to the energy-penetration curve of the reference collision scenario (see Figure 10). However, the central energy value of the simulation occurs at 70.2MJ, an energy level greater than the reference ship internal energy (46.05MJ) at the onset of outer hull fracture. This highlights the possibility of one or more simulated ship-iceberg collision scenarios having higher penetration distance that can lead to hull rupture. The exceedance of the mean energy confirms the importance of assessing the performance of ship structures in collisions.

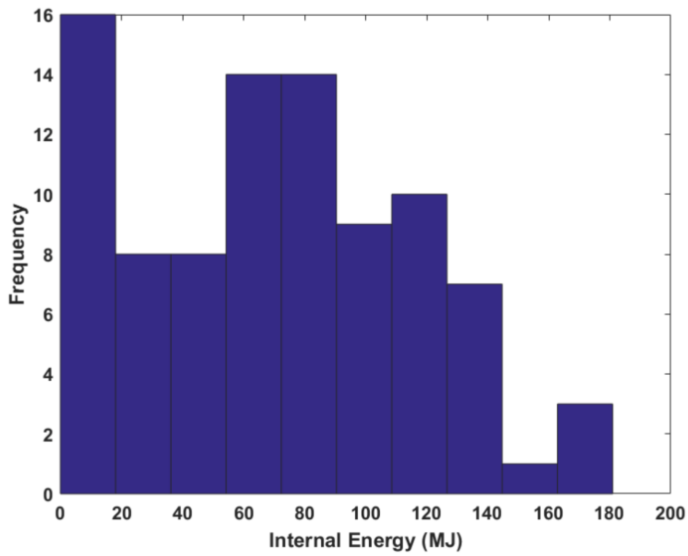

Figure 12. Energy distribution of collision scenario simulations.

5.2 Surrogate model evaluation

The mathematical relationship between the input random variables and struck ship response are evaluated using the Kriging surrogate model. The kriging models use the method of interpolation based on the assumption that there is a spatial correlation between the model predictions. The models have been proven to be useful in the approximation of both deterministic and stochastic simulations by fitting explicit functions to their predefined input and the corresponding output data [59, 60]. The kriging model estimates the value of a predictor from the sum of the weighted value of the surrounding (known) samples. The associated values of these known samples are functions of the random variables and are evaluated from the aforementioned deterministic or stochastic simulations. Hence, the basic form of Kriging predictor for the prediction of values is [61, 62]:

$$\boldsymbol{Y}(\boldsymbol{X}) - f(\boldsymbol{X}) = \boldsymbol{\Psi}^{-1}\boldsymbol{r}[\boldsymbol{Y}(\boldsymbol{X}') - f(\boldsymbol{X}')], \tag{19}$$

where $\boldsymbol{X}$ **and** $\boldsymbol{X}'$ are the point location vectors for the predictor point and the surrounding data points, respectively (note that these locations are determined by the input design sets); $f(\boldsymbol{X})$ and $f(\boldsymbol{X}')$ are the regression functions and are the mean of the broader simulation outputs $\boldsymbol{Y}(\boldsymbol{X})$ and $\boldsymbol{Y}(\boldsymbol{X}')$, respectively. In some Kriging variants, the regression function is a constant (e.g. an unknown constant in ordinary Kriging and zero in simple Kriging). The parameters, $\boldsymbol{\Psi}^{-1}$ and $\boldsymbol{r}$ are correlation matrices representing the distance between surrounding data point pairs and the distance between data points and the predictor point, respectively. The product of the two matrices is known as the *kriging weight*. Readers are directed to Obisesan and Sriramula [21] for more details about the correlation matrices. Based on the knowledge of the kriging weight, it can be shown that a predictor evaluated at a known location x' will be equal to the observed simulation output hence, the kriging predictor is an 'exact' interpolator. In the present study, the Kriging model procedure is evaluated using MATLAB®.

Due to the consideration of a high number of random variables and the correlation between the variables, the mathematical expressions derived from the Kriging modelling process are too large to be displayed in the study. However, the model accuracy is assessed by comparing its result with those derived from sampling the ACM with 10 input design sets, presented in Table 5. A scatter plot of the internal energy predicted by the Kriging model and that observed from the ACM is shown in Figure 13. It can be seen that the Kriging model provides an accurate approximation of the struck ship response in iceberg collisions. The accuracy of the Kriging model is further assessed by plotting its residual against the energy values observed from the ACM, as shown in Figure 14. The mean, minimum and maximum percentage error of the Kriging model are estimated to be 1.150%, 0.33% and 4.67%, respectively. Hence, the developed surrogate model is adequate for predicting the stochastic response of the reference ship in iceberg collisions.

Table 5. Input design sets for validation of Kriging surrogate model.

Sets	$M_{ice}(kt)$	$v_{ice}(m/s)$	$\Delta_{ship}(kt)$	$v_{ship}(m/s)$	$\theta(rad)$	I_l	$D_{ship}(m)$
1	17.8580	0.1595	65.7801	3.7646	0.3773	0.3204	18.9820
2	52.9407	0.0800	99.3865	2.4062	0.6175	0.5847	19.5097
3	12.0370	0.7832	75.8881	2.7439	0.8693	0.4134	19.2587
4	53.5471	0.0682	127.5361	2.2995	1.1448	0.5104	19.0411
5	18.6081	0.8011	62.1387	3.4605	1.3759	0.6821	19.4454
6	8.2878	0.1383	106.2482	1.7964	1.6323	0.1272	19.5009
7	48.6197	0.3213	104.3579	2.5248	1.9042	0.3092	18.6528
8	47.5356	0.4909	119.0119	1.1743	2.1474	0.3296	19.0811
9	66.6307	0.4449	77.6042	3.1942	2.3883	0.8647	19.4285
10	33.7330	0.6063	72.1313	2.1375	2.6652	0.6024	17.5560

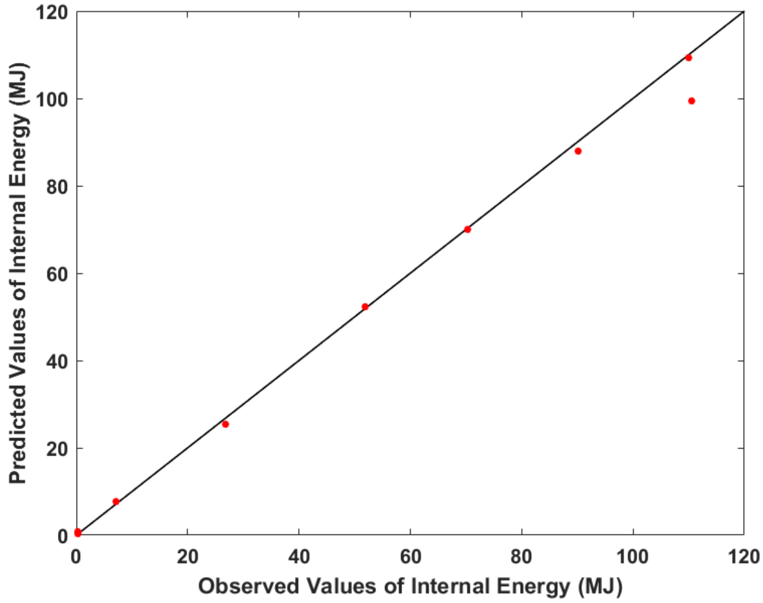

Figure 13. Scatter plot of the predicted and observed energy values.

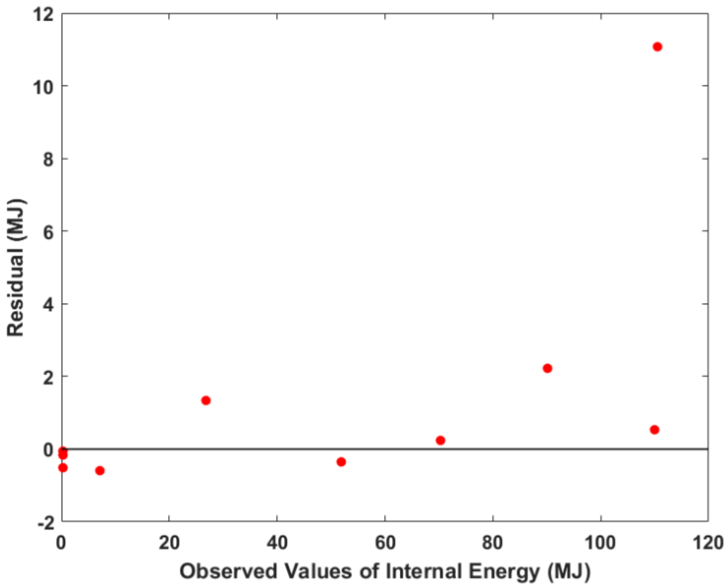

Figure 14. Residual plot of Kriging models for the reference struck ship.

6. QUANTITATIVE RISK ASSESSMENT

As discussed in Section 1, assessing the asset risk associated with the double-hull crude oil carrier requires the evaluation of its two key components; the probability of damage to the structure and related consequences (see Equation 1). The consequence considered in the present study is defined as the rupture of the asset that is, the reference double-hull oil tanker, which could lead to flooding of the damaged compartment. Since asset risk is considered, the evaluated structural responses of the reference ship from Section 3 are direct representatives of the consequence component of the risk computation. The evaluation of the probability of damage and that of collision are discussed in this section followed by the computation of the asset risk in relation to the reference ship.

6.1 Evaluation of $\boldsymbol{P(Collision)}$

The probability of a ship-iceberg collision is estimated in the present study from the following equation [44]:

$$P(Collision) = 1 - e^{-F_{ship-iceberg}}, \tag{20}$$

$$F_{ship-iceberg} = P_c N_e \,, \tag{21}$$

where N_e is the expected number of icebergs encountered per ship year and P_c is the causation probability. Two models have been found so far in the literature for estimating N_e; the Iceberg Drift (ID-model) and Swept area (SA-model). Both models are evaluated based on iceberg detection and management within a certain area and time period with respect to the environmental conditions present. The ID-model involves the numerical modelling of iceberg trajectories with respect to their motion and deterioration over a period of time [25]. The SA-model provides a theoretical approach to estimating N_e by estimating the areal density of icebergs from the integral of their marginal probabilities [63]. Hence, N_e can be estimated from the following equation:

$$N_e = \rho(D_{col} + \overline{W}_{ice})\bar{v}_{ice}T, \tag{22}$$

$$\rho = \frac{n_{ice}.T_r}{A}, \tag{23}$$

where ρ is the average areal density of icebergs measured as the number of icebergs per m^2, n_{ice} is the iceberg frequency per year, A is the observed regional area, T_r is the iceberg residence period in the regional area per year, D_{col} is the collision diameter, $\overline{W}_{ice}$ is the mean iceberg width, $\bar{v}_{ice}$ is the average iceberg drift velocity and T is the time period in seconds. The

SA-model is chosen for N_e estimation in the present study as the ID-model would be computationally expensive. Although the SA-model is estimated for encounter scenarios, the model is limited in this approach as parameters describing collision avoidance procedures and hydrodynamic effect on icebergs are assumed to be negligible. The study by Eik and Gudmestad [25] assessed iceberg impacts within the Shtokman region with an observed iceberg frequency of 880 in 100-year period. The icebergs were assumed to have equal residence time of 5 days within the $73105 \times 10^6 m^2$ region. The diameter of collision circle is assumed to be $1000\ m$ while the mean iceberg width is $90\ m$. These data along with those of the reference collision scenario described in Section 3 are used in the study to evaluate $\mathrm{N_e}$. By applying these data into Equation 22 and Equation 23, ρ is evaluated as $1.649 \times 10^{-12}\ iceberg/m^2$ thus, the number of icebergs encountered per ship year is derived as 0.017.

The causation probability (P_c) is estimated by capturing the logic of the chain of actions, inactions and external contributions leading to the accident. Fault tree analysis (FTA) is applied in the present study by linking uncorrelated events in Boolean algebra using OR- and AND- logic gates. The probability of the output from the logic gates are evaluated using the following equations:

$$P_{OR}(Occurence) = 1 - \prod_i (1 - p_i), \tag{24}$$

$$P_{AND}(Occurence) = \prod_i p_i, \tag{25}$$

where p_i is the probability of the input events to the logic gates. The proposed fault tree model is presented in Figure 15. To estimate the top event (P_c), the failure probability of basic events are assigned and used for evaluating the intermediate events leading up to the top event. Basic event probabilities are defined from corresponding values available in the literature and opinion of experts for various kinds of ship accident assessments [8, 47, 63, 65, 66]. For example, occurrence probability of the high wave event is estimated using the Weibull distribution with shape and scale parameters of 2 and 1.48, respectively, with extreme wave height probability analysed at $3m$ and above [66]. A brief description and value of the basic, intermediate and top events of the FTA is provided in Table 6. The event of encountering floe-bergs is included in the probability estimation because these heavily hummocked ice pack may pose hazards, like those from icebergs, to ships navigating ice-infested waters. The basic events are assumed to be statistically independent in this study. However, it should be noted that some of the considered events could be correlated in reality. By applying Boolean logic evaluations, P_c for ship-iceberg collisions is derived as 1.2×10^{-5}.

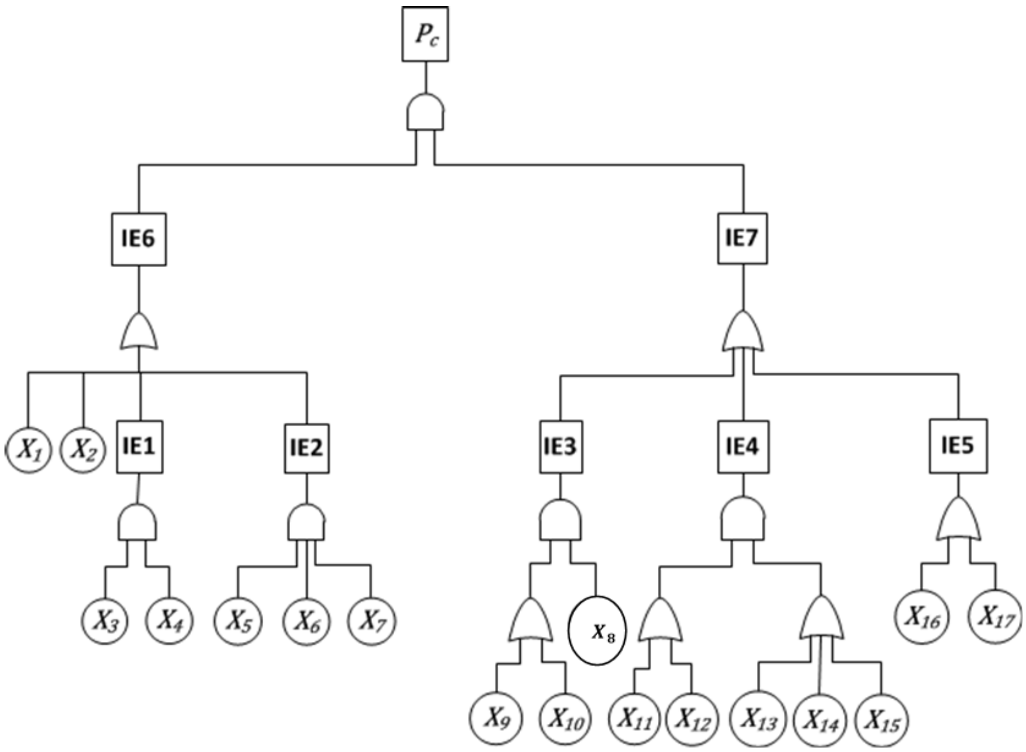

Figure 15. Fault tree model for ship-iceberg causation probability estimation.

Table 6. Description and value of fault tree events.

Index	Event description	Occurrence probability	Reference
$X1$	Faults from other ships	4.2×10^{-5}	[65]
$X2$	Ice breaker failure	5.7×10^{-4}	[8]
$X3$	Waning sea ice	1.0×10^{-3}	[8]
$X4$	Wave	2.3×10^{-3}	[8]
$IE1$	Drifting icebergs	2.3×10^{-6}	
$X5$	Floe formation	5.3×10^{-3}	[8]
$X6$	Sea current	7.7×10^{-2}	[67]
$X7$	High wind	1.7×10^{-3}	[8]
$IE2$	Floe-bergs	6.9×10^{-7}	
$X8$	High speed	7.0×10^{-4}	[8]
$X9$	Equipment failure	4.5×10^{-6}	[65]
$X10$	Human error	1.4×10^{-4}	[65]
$IE3$	Navigation error	9.9×10^{-8}	
$X11$	Human error	1.4×10^{-4}	[65]
$X12$	Radar failure	1.0×10^{-3}	[8]
$X13$	Fog	5.0×10^{-3}	[8]
$X14$	High wind	1.7×10^{-3}	[8]
$X15$	Physical obstacle	1.0×10^{-2}	[8]
$IE4$	Poor visibility	1.8×10^{-5}	
$X16$	High winds	1.7×10^{-3}	[8]
$X17$	High waves	1.7×10^{-2}	[66]
$IE5$	Bad weather (sea state)	1.9×10^{-2}	
$IE6$	Potential ice obstacle	6.2×10^{-4}	
$IE7$	Ship on collision course	1.9×10^{-2}	
P_c	Ship-iceberg collision	$\mathbf{1.2 \times 10^{-5}}$	

6.2 Evaluation of $P(Damage|Collision)$

Surrogate models derived from the use of the Kriging interpolations are combined with First and Second Order Reliability Methods (FORM/SORM) to evaluate $P(Damage|Collision)$. The objective of the present structural reliability analysis is to assess the performance of the double-hull oil tanker with respect to the studied collision scenario. The analysis is done by the definition of a limit state function (LSF) expressed as $G(\boldsymbol{X})$. The LSF is the difference between the capacity and the load a structure will be exposed to. In order to align the LSF of the present study with the objective of the structural reliability analysis, capacity is characterised as the energy value from the damage assessment of the reference collision scenario at the onset of outer hull fracture (46.05MJ, see Section 3). Hence, the structural reliability assessment is performed with the consideration of as-design hull rupture criteria. Surrogate models, in conjunction with the probabilistic characteristics of the input random variables, are used to evaluate the load component of the LSF. From the definition of the capacity and load components of the LSF, the evaluation of the probability of occurrence of damage given a ship-iceberg collision is performed by comparing the energy value of the reference ship at the onset of outer hull fracture with energy values at the end of probable ship-iceberg collision events. Mathematically, the probability of the occurrence of an event can be estimated as:

$$P(f) = P[G(\boldsymbol{X}) \leq 0] = \int_{G(\boldsymbol{X})\leq 0} f_{\boldsymbol{X}}(\boldsymbol{X}) d\boldsymbol{X}, \quad (26)$$

where $f_{\boldsymbol{X}}(\boldsymbol{X})$ is the joint probability density function of the $n-$dimensional vector of the random variable $\boldsymbol{X}$. The solution to Equation 26 can be achieved from the iterative numerical techniques [68]. The Finite Element Reliability Using MATLAB® (FERUM) version 4.1 developed by Bourinet et al. [69] is used to analyse the structural reliability using the FORM and SORM methods. Results of the reliability analysis show that the probability of hull rupture given the ship-iceberg collision $[P(Damage|Collision)]$ is 0.5536. This suggests that there is approximately a 55% chance of the reference ship outer hull rupturing when in an iceberg collision. The failure probability result can be combined with other risk components, collision probability and consequence, to support decisions on the design process of the reference ship in risk-based designs. Outcomes of the reliability analysis quantify the sensitivity of the probability result on the input random variables and provide the most probable design value of the random variables. The evaluated sensitivity index of the random variables are presented in Table 7. The sensitivity analysis shows the collision angle to be the most influential variable on the probability result, followed by the reference ship displacement. Iceberg mass appears to be relatively insignificant to the probability estimation and this may be because change in iceberg velocities during the collision process are not represented in the present model. Aside from the magnitude of the sensitivity indices, the analysis also shows the direction at which the design values of the random variables can be adjusted; a random variable with a negative sensitivity index means that the design value could be reduced while that which is positive signifies value increase for the purpose of improving the reliability of the reference struck ship in ship-iceberg collisions.

The most probable design values of the random variables are also presented in Table 7. These values are critical to ship designers as they can serve as the reference design values of the random variables that can be adjusted to improve the reliability of the reference ship in collisions. The most probable design values derived in the study are particular to the framework utilised to characterise the performance of the reference ship. With the reliability analysis result, all elements required to assess the asset risk of the reference ship are available and the risk is evaluated as:

$$Risk = P(Damage|Collision) \times 1 - e^{-F_{ship-iceberg}} \times Consequence \,, \qquad (27)$$

$$Risk = 0.5536 \times 1 - e^{-(1.2\times10^{-5}\times0.017)} \times 46.05 \times 10^{6} \qquad (28)$$

$$= 5.2006 \ \text{J/ship year.}$$

Within the context of the present study, it is observed that the key components that influence the computed risk value are the order of magnitude of the consequence measure and the conditional probability estimated from reliability analysis; the power of 10 from the consequence measure approximately strikes out the estimated value of $P(Collision)$. Hence, an increased reliability of the ship structure will result in a reduced risk to the ship in iceberg collisions. Likewise, a reduced damage to the ship structure will also translate to a reduced risk computation. The risk result also indicates that the use of energy as a performance metric may be unsuitable as it undermines the influence of probability parameters in the equation of risk. Other performance metrics that relate to the extent of structural damage are recommended as suitable metrics for the assessment of ship structural performance in ship-iceberg collisions. Example of such metrics could be the structural damaged volume and iceberg penetration. However, the computed risk tends to serve as a guideline by indicating the component of risk computation that requires more focus during risk-based design. It should be noted that there are some factors from the estimation of the collision probability that could influence risk computation such as parameters of the shipping route considered and quantified values of basic events leading up to the evaluation of the causation probability. With the identification of reliability and consequence parameters as key parameters influencing the evaluated risk value, the measure of performance of ship structures can be further improved against future ship-iceberg collisions.

Table 7. Performance measures for the reference ship based on FORM analysis.

Hasofer-Lind index, $\beta = -0.1348$ $P[G(S,R) \leq 0] = 0.5536$							
Parameters	$\boldsymbol{M_{ice}}$	$\boldsymbol{v_{ice}}$	$\boldsymbol{\Delta_{ship}}$	$\boldsymbol{v_{ship}}$	$\boldsymbol{\theta}$	$\boldsymbol{I_l}$	$\boldsymbol{D_{ship}}$
Sensitivity index ($\boldsymbol{\alpha}$)	0.0040	0.0608	0.4751	0.0065	-0.8768	0.0404	-0.0105
Design value	$35.6760\ t$	$0.2499\ m/s$	$97.4370\ t$	$2.8279\ m/s$	$1.5515\ rad$	0.5256	$18.8333m$

7. CONCLUSIONS

The transferability of the stochastic performance characterisation model framework for ship-ship collisions is proven in this study by the application to ship-iceberg collisions. The framework was demonstrated by characterising the response of the reference double-hull tanker in collision with a spherical iceberg. A number of collision scenarios were defined using input random variables that influence collision response. A simplified model of the computationally intensive finite element model was captured using the Kriging response surface model.

Parameters of crushable foam plasticity model were evaluated from available data for ice triaxial tests to model the iceberg material. The validation of the model with the recommended ISO pressure-area curve showed good agreement, especially at contact areas greater than $0.5m^2$.The model was applied to the simulation of the reference ship-iceberg collision scenario for the evaluation of response values at specified simulation period. Both the iceberg and the reference ship were observed to contribute to the total dissipated energy of

93.54MJ by 33% and 67%, respectively. The outer hull of the reference ship was observed to rupture at internal energy beginning from 46.05MJ.

The propagation of 90 input design sets, generated using LHS, through an automated finite element model of the reference collision scenario resulted in the corresponding internal energy responses between 1361.63J and 180.93MJ with the recorded internal energy occurring mostly between 0 and 20MJ. The Kriging response surface model was used to evaluate a surrogate model for the input-response relationship. The Kriging model provided a good approximation of the stochastic response of the reference ship with mean and maximum percentage error of 1.150% and 4.67%, respectively.

The probability of ship-iceberg collision $[P(Collision)]$ was obtained from fault tree analysis (FTA) by linking identified basic events leading up to the collision event. The causation probability was estimated as 1.2×10^{-5}. The number of possible ship-iceberg collisions(N_e) for the Shtokman region was evaluated using the Swept area model available in the literature. The number was estimated as 0.017 icebergs per ship year. FORM and SORM analyses performed with the use of the developed Kriging model estimated $P(Damage|Collision)$ as 0.5536. The evaluation of these risk components, $P(Collision)$, N_e and $P(Damage|Collision)$ were used to compute the asset risk to the reference ship due to iceberg collision and this was estimated in energy terms as 5.2006 joules per ship year. Further improvements are needed to the probabilistic quantification of input variables in the proposed framework as information on ship-ship collisions were used in cases where there is no available data for ship-iceberg collision scenarios.

For the purpose of improving the reliability of ship structures in collisions, results of sensitivity analysis and the most probable design values from FORM analysis were discussed. Collision angle was found to be the most sensitive random variable to $P(Damage|Collision)$ estimation with an index of -0.9065. The variability of iceberg mass appeared to be insignificant to the probability estimation and this could be affected by the fact that the change in iceberg speed during collision analysis was not considered for the numerical simulations. The change in iceberg speed may be very important to the evaluation of the ship structural response and offers a valuable opportunity to extend the proposed framework. The most probable design points of the input random variables were identified and they can serve as reference design values for ship designers to improve the ship structural reliability. These design values may vary with the choice of performance functions and probabilistic characterisation of identified input parameters of assessed collision scenario. The proposed framework provides a valuable tool for optimal performance characterisation and risk-based design of ships navigating in the Arctic waters. The framework can be easily extended to characterise the performance and risk of ship structures other than the double-hull oil tanker presented in the study.

ACKNOWLEDGEMENTS

The authors are grateful for the support provided through the Lloyd's Register Foundation Centre. The Foundation helps to protect life and property by supporting engineering-related education, public engagement and the application of research.

REFERENCES

[1] Suh, Y., Ito, H., Chun, S., Han, S., Choi, J. and Urm, H., (2008). Ice Collision Analyses for Membrane Tank Type LNG Carrier, **12(1)** pp.35-44.

[2] Leira, B., Børsheim, L., Espeland, Ø. and Amdahl, J., (2009). Ice-load estimation for a ship hull based on continuous response monitoring, *Proceedings of the Institution of Mechanical Engineers Part M: Journal of Engineering for the Maritime Environment,* **223** (4), pp.529-540.

[3] Youssef, S.A.M., Paik, J.K., Kim, Y.S., Kim, M.S. and Cheng, F., (2013). Probabilistic selection of ship-ship collision scenarios, *Proceedings of the International Conference on Offshore Mechanics and Arctic Engineering - OMAE,* Nantes, France, June 9-14 2013,

[4] Fuglem, M., (1997). *Decision-Making for Offshore Resource Development [PhD Thesis],* PhD. Memorial University of Newfoundland

[5] IMO, (2007). *Formal safety assessment - liquefied natura gas (LNG) carriers,* Report No. MSC83/INF.3, London: International Maritime Organization.

[6] Reddy, D.V., Arockiasamy, M., Cheema, P.S. and Riggs, N.P., (1980). Monte Carlo simulation of iceberg impact probabilities, *Cold Regions Science and Technology,* **1** (3-4), pp.293-297.

[7] Korsnes, R., (1989). Long-term iceberg collision-risk assessment methods for fixed offshore structures, *Probabilistic Engineering Mechanics,* **4** (4), pp.203-214.

[8] Khan, F., Yang, M., Veitch, B., Ehlers, S. and Chai, S., (2014). Transportation risk analysis framework for arctic waters, *Proceedings of the International Conference on Offshore Mechanics and Arctic Engineering - OMAE,* San Francisco, California, June 8-13, 2014,

[9] NORSOK, (2004). *Design of steel structures,* Report No. N-004, Standards Norway: NORSOK.

[10] Wang, J.Y. and Derradji-Aouat, A., (2010). *Ship performance in broken ice floes - preliminary numerical simulations,* Report No. TR-2010-24, St. John's, NL, Canada: Institute for Ocean Technology, National Research Council.

[11] Song, M., Kim, E., Amdahl, J., Greco, M. and Souli, M., (2016). "Numerical investigation of fluid-ice-structure interaction during collision by an arbitrary langragian eulerian method", *ASME 2016 35th International Conference on Ocean, Offshore and Arctic Engineering,* Busan, South Korea, June 19-24, 2016, pp. 1-8.

[12] Fredriksen, Ø., (2012). *Ice-Induced Loading on Ship Hull During Ramming [Master Thesis],* Masters. Norwegian University of Science and Technology

[13] Liu, Z., Amdahl, J. and Løset, S., (2011). Plasticity based material modelling of ice and its application to ship-iceberg impacts, *Cold Regions Science and Technology,* **65** (3), pp.326-334.

[14] Gao, Y., Hu, Z., Ringsberg, J.W. and Wang, J., (2015). An elastic-plastic ice material model for ship-iceberg collision simulations, *Ocean Engineering,* **102** pp.27-39.

[15] Daley, C. and Kim, H., (2010). Ice collision forces considering structural deformation, *Proceedings of the International Conference on Offshore Mechanics and Arctic Engineering - OMAE,* Shanghai, China, June 6-11, 2010, pp. 817-825.

[16] Friis-Hansen, P. and Simonsen, B.C., (2002). GRACAT: software for grounding and collision risk analysis, *Marine Structures,* **15** (4–5), pp.383-401.

[17] Brown, A.J., (2002). Collision scenarios and probabilistic collision damage, *Marine Structures*, **15** (4-5), pp.335-364.

[18] Paik, J.K. and Pedersen, P.T., (1996). Modelling of the internal mechanics in ship collisions, *Ocean Engineering*, **23** (2), pp.107-142.

[19] Abramowicz, W. and Sinmao, M., (1999). *User's manual and modeling guide for the program DAMAGE, v. 4.0, joint MIT-industry program on tanker safety,* Report No. 66, Cambridge, MA: Department of ocean engineering MIT.

[20] Liu, Z., Garrè, L. and Amdahl, J., (2011). Analysis of foreship and iceberg impact loads based on bayesian networks, *Proceedings of the International Conference on Offshore Mechanics and Arctic Engineering - OMAE*, Rotterdam, The Netherlands, June 19-24, 2011, pp. 965-974.

[21] Obisesan, A. and Sriramula, S., (2017). Performance Characterisation for Risk Assessment of Striking Ship Impacts Based on Struck Ship Damaged Volume, *Journal of Marine Science and Application*, **16** (2), pp. 111-128.

[22] Quinton, B.W.T., Daley, C.G. and Gagnon, R.E., (2012). Realistic moving ice loads and ship structural response, *Proceedings of the International Offshore and Polar Engineering Conference*, Rhodes, Greece, June 17-22 2012, pp. 1208-1214.

[23] Lu, P., Li, Z., Shi, L. and Huang, W., (2013). Marine radar observations of iceberg distribution in the summer Southern Ocean, *Annals of Glaciology*, **54** (62), pp.35-40.

[24] Romanov, Y.A., Romanova, N.A. and Romanov, P., (2012). Shape and size of Antarctic icebergs derived from ship observation data, *Antarctic Science*, **24** (1), pp.77-87.

[25] Eik, K. and Gudmestad, O.T., (2010). Iceberg management and impact on design of offshore structures, *Cold Regions Science and Technology,* **63** (1-2), pp.15-28.

[26] Obisesan, A., Sriramula, S. and Harrigan, J., (2015). A framework for reliability assessment of ship hull damage under ship bow impact, *Ships and Offshore Structures*, (10.1080/17445302.2015.1051281),

[27] Zhang, S., (1999). *The mechanics of ship collisions [PhD Thesis]*, Technical University of Denmark

[28] Haris, S. and Amdahl, J., (2012). An analytical model to assess a ship side during a collision, *Ships and Offshore Structures*, **7** (4), pp.431-448.

[29] Wang, G., Ohtsubo, H. and Arita, K., (1998). Large deflection of a rigid-plastic circular plate pressed by a rigid sphere, **65** pp.533-533-535.

[30] Jones, S.J., (1982). The confined compressive strength of polycrystalline ice. *Journal of Glaciology*, **28** (98), pp.171-177.

[31] Gagnon, R.E. and Gammon, P.H., (1995). Triaxial experiments on iceberg and glacier ice, *Journal of Glaciology,* **41** (139), pp.528-540.

[32] Løset, S., (1993). Thermal Energy Conservation in Icebergs and Tracking by Temperature, **98** (C6), pp.10001–10012.

[33] Derradji-Aouat, A., (2000). A unified failure envelope for isotropic fresh water ice and iceberg ice, *ETCE/OMAE 2000 Joint Conference,* New Orleans, Louisiana, February 14-17, 2000,

[34] Derradji-Aouat, A., Sarzynski, M. and Cordes, R., (2015). Iceberg ice constitutive modeling and FEA validation, *Presented at the Arctic Technology Conference,* Copenhagen, Denmark, March 23 2015,

[35] Gagnon, R.E., (2007). Results of numerical simulations of growler impact tests, *Cold Regions Science and Technology,* **49** (3), pp.206-214.

[36] Gagnon, R.E., (2011). A numerical model of ice crushing using a foam analogue, *Cold Regions Science and Technology,* **65** (3), pp.335-350.

[37] Fish, A.M. and Zaretsky, Y.K., (1998). Strength and creep of ice in terms of mohr-coulomb fracture theory, *Proceedings of the Eight International Offshore and Polar Engineering Conference,* Montreal, Canada, May 24-29 1998, pp. 416-424.

[38] Gao, Y., Hu, Z. and Wang, J., (2014). Sensitivity Analysis for Iceberg Geometry Shape in Ship-Iceberg Collision in View of Different Material Models, **2014** pp.1-11.

[39] Dassault Systèmes, *ABAQUS 6.11 analysis user's manual,* Report No. Online Documentation Help,

[40] Singh, S.K. and Jordaan, I.J., (1996). Triaxial tests on crushed ice, *Cold Regions Science and Technology,* **24** (2),

[41] Kim, H., Daley, C. and Colbourne, B., (2015). A numerical model for ice crushing on concave surfaces, *Ocean Engineering,* **106** pp.289-297.

[42] Karr, D.G. and Choi, K., (1989). A three-dimensional constitutive damage model for polycrystalline ice, *Mechanics of Materials,* **8** (1),

[43] ISO/CD 19906, *Petroleum and natural gas industries — arctic offshore structures,* Report No. ISO TC 67/SC 7/WG 8.

[44] Lutzen, M., (2001). *Ship Collision damage [PhD dissertation]*, Department of Mechanical Engineering, Technical university of Denmark.

[45] DNV, (2006). *Ice collision scenario,* Report No. 2006-0672, Det Norske Veritas.

[46] McKenna, R., (2005). Iceberg shape characterization, *Proceedings of the International Conference on Port and Ocean Engineering under Arctic Conditions, POAC,* Potsdam, NY, January 2005, pp. 555-564.

[47] Fuglem, M., Muggeridge, K. and Jordaan, I., (1999). Design load calculations for iceberg impacts, *International Journal of Offshore and Polar Engineering,* **9** (4), pp.298-306.

[48] Neshyba, S., (1980). Iceberg Dynamics Symposium On the size distribution of Antarctic icebergs, *Cold Regions Science and Technology,* **1** (3),

[49] Ralph, F., Jordaan, I., Clark, P. and Stuckey, P., (2006). *Estimating probabilistic iceberg design loads on ships navigating in ice,* **ICETECH06-141-RF**pp.February 2016-1-7.

[50] Storheim, M., Kim, E., Amdahl, J. and Ehlers, S., (2012). Iceberg shape sensitivity in ship impact assessment in view of existing material models, *Proceedings of the International Conference on Offshore Mechanics and Arctic Engineering - OMAE,* Rio de Janeiro, Brazil, July 1-6, 2012, pp. 507-517.

[51] Wang, B., Yu, H. and Basu, R., (2008). Ship and ice collision modeling and strength evaluation of LNG ship structure, *ASME 27th International Conference on Offshore Mechanics and Arctic Engineering,* Estoril, Portugal, June 15-20 2008,

[52] Kim, E., Storheim, M., Von Bock Und Polach, R. and Amdahl, J., (2012). Design and modelling of accidental ship collisions with ice masses at laboratory-scale, *Proceedings of the International Conference on Offshore Mechanics and Arctic Engineering - OMAE,* Rio de Janeiro, Brazil, July 1-6, 2012, pp. 495-505.

[53] Ying Wei Liu and Moses, F., (1994). A sequential response surface method and its application in the reliability analysis of aircraft structural systems, *Structural Safety,* **16** (1-2), pp.39-46.

[54] Haldar, A. and Mahadevan, S., (2000). Reliability Assessment using Stochastic Finite Element Analysis. New York: John Wiley & Sons, Inc.

[55] Kaymaz, I. and McMahon, C.A., (2005). A response surface method based on weighted regression for structural reliability analysis, *Probabilistic Engineering Mechanics,* **20** (1), pp.11-17.

[56] Myers, R.H., Montgomery, D.C. and Anderson-Cook, C.M., (2009). Response Surface Methodology: Process and Product Optimization using Designed Experiments. USA: Hoboken, N.J.: Wiley.

[57] Mckay, M.D., Beckman, R.J. and Conover, W.J., (2000). A comparison of three methods for selecting values of input variables in the analysis of output from a computer code, *Technometrics,* **42** (1), pp.55-61.

[58] Tang, B., (1993). Orthogonal array-based latin hypercubes, *Journal of the American Statistical Association,* **88** (424), pp.1392-1397.

[59] Couckuyt, I., Dhaene, T. and Demeester, P., (2013). *ooDACE toolbox - A Matlab Kriging Toolbox: Getting started*, Available at: http://sumowiki.intec.ugent.be/OoDACE:ooDACE_toolbox

[60] Lophaven, S.N., Nielsen, B.N. and Sondergaard, J., *DACE - A matlab kriging toolbox, version 2.0,* Report No. IMM-REP-2002-12,

[61] Bohling, G., (2005). *Kriging*, Available at: http://people.ku.edu/~gbohling/cpe940/Kriging.pdf

[62] Kleijnen, J.P.C., (2009). Kriging metamodeling in simulation: A review, *European Journal of Operational Research,* **192** (3), pp.707-716.

[63] Fuglem, M., Jordaan, I., Crocker, G., Cammaert, G. and Berry, B., (1996). Environmental factors in iceberg collision risks for floating systems, *Cold Regions Science and Technology,* **24** (3), pp.251-261.

[64] Valdez Banda, O.A., Goerlandt, F., Montewka, J. and Kujala, P., (2015). A risk analysis of winter navigation in Finnish sea areas, *Accident Analysis and Prevention*, **79** pp.100-116.

[65] Li, S., Meng, Q. and Qu, X., (2012). An Overview of Maritime Waterway Quantitative Risk Assessment Models, *Risk Analysis,* **32** (3), pp.496-512.

[66] Khon, V. C., I. I. Mokhov, F. A. Pogarskiy, A. Babanin, K. Dethloff, A. Rinke, and H. Matthes (2014). Wave heights in the 21st century Arctic Ocean simulated with a regional climate model, Geophys. Res. Lett., 41, 2956–2961, doi:10.1002/2014GL059847.

[67] Ashkenazy, Y. and Gildor, H., (2011). On the probability and spatial distribution of ocean surface currents, *Journal of Physical Oceanography,* **41** (12), pp.2295-2306.

[68] Ditlevsen, O. and Madsen, H.O., (2007). Structural Reliability Methods. Chichester: John Wiley & Sons Ltd.

[69] Bourinet, J.M., Mattrand, C. and Dubourg, V., (2009). A review of recent features and improvements added to FERUM software, *10th International Conference on Structural Safety and Reliability (ICOSSAR 2009),* Osaka, Japan, September 2009.